Biochimica et Biophysica Acta 1847 (2015) 587–598

Contents lists available at ScienceDirect

Biochimica et Biophysica Acta

journal homepage: www.elsevier.com/locate/bbabio

Cardiolipin is a key determinant for mtDNA stability and segregation during mitochondrial stress

Luis Alberto Luévano-Martínez *, Maria Fernanda Forni, Valquiria Tiago dos Santos, Nadja C. Souza-Pinto, Alicia J. Kowaltowski

Departamento de Bioquímica, Instituto de Química, Universidade de São Paulo, Cidade Universitária, Av. Prof. Lineu Prestes, 748, São Paulo, SP 05508-000, Brazil

ARTICLE INFO

Article history:
Received 2 January 2015
Received in revised form 16 March 2015
Accepted 29 March 2015
Available online 2 April 2015

Keywords:
Phospholipid
Mitochondrion
Mitochondrial DNA
Membrane plasticity

ABSTRACT

Mitochondria play a key role in adaptation during stressing situations. Cardiolipin, the main anionic phospholipid in mitochondrial membranes, is expected to be a determinant in this adaptive mechanism since it modulates the activity of most membrane proteins. Here, we used *Saccharomyces cerevisiae* subjected to conditions that affect mitochondrial metabolism as a model to determine the possible role of cardiolipin in stress adaptation. Interestingly, we found that thermal stress promotes a 30% increase in the cardiolipin content and modifies the physical state of mitochondrial membranes. These changes have effects on mtDNA stability, adapting cells to thermal stress. Conversely, this effect is cardiolipin-dependent since a cardiolipin synthase-null mutant strain is unable to adapt to thermal stress as observed by a 60% increase of cells lacking mtDNA (ρ^0). Interestingly, we found that the loss of cardiolipin specifically affects the segregation of mtDNA to daughter cells, leading to a respiratory deficient phenotype after replication. We also provide evidence that mtDNA physically interacts with cardiolipin both in *S. cerevisiae* and in mammalian mitochondria. Overall, our results demonstrate that the mitochondrial lipid cardiolipin is a key determinant in the maintenance of mtDNA stability and segregation.

1. Introduction

Phospholipids are components of all cellular structures. Most, including PC, are synthesized in the lumen of the endoplasmic reticulum and subsequently distributed intracellularly [1]. Non-bilayer phospholipids such as CL and PE are synthesized mainly in mitochondria, where they also exert their functions [2]. After synthesis, PE is distributed through all cellular membranes, where it exerts diverse functions such as autophagy [3] or signal transduction [4].

CL is the main anionic phospholipid in mitochondrial membranes, where it constitutes about 15% of the total phospholipid content. It is synthesized in the inner leaflet of the inner membrane and remains within mitochondria, and distributed throughout the inner membrane [5], where it confers the negative surface charge necessary to maintain a localized proton motive force, used to synthesize ATP [6]. Furthermore, CL participates in the biogenesis and assembly of respiratory chain components and several metabolite transporters [7]. Functionally, CL activates the adenine nucleotide translocator (ANT) and uncoupling protein 1 (UCP1; [8,9]).

Additionally, CL stabilizes F_1F_O-ATP synthase dimers [10] and respiratory chain supercomplexes [11], affecting mitochondrial morphology [12]. CL normally adopts a bilayer conformation, but when calcium is present in the interface, it assumes a conical inverted shape due to the low hydration of the small polar headgroup [13]. Interestingly, it has been recently demonstrated that CL is able to respond to the chemical component of the proton motive force, promoting the formation of cristae-like structures in the inner membrane [14], an effect that resembles that of calcium on CL-containing membranes.

In bacteria, both CL and its precursor, PG, are key elements in the response which confers resistance to osmotic and thermal stresses [15]. Moreover, anionic phospholipids are necessary to attract and stabilize the translational machinery during the synthesis of hydrophobic proteins [16]. Since mitochondria are ancestrally related to bacteria, these mechanisms may have been conserved throughout evolution. Indeed, studies have shown that the loss of cardiolipin results in elevated sensitivity to thermal stress, including loss of viability, mitochondrial DNA, changes in mitochondrial bioenergetics, mitochondrial protein import,

Abbreviations: NBD-PE, 1,2-oleyl-sn-glycero-3-phosphoethanolamine-N-7-nitro-2-1,3-benzoxadiazol-4-yl; ANSA, 1-anilino-8-naphthalenesulfonic acid; HEPES, 4-[2-hydroxyethyl]-1-piperazineethanesulfonic acid; DAPI, 4′,6-diamidino-2-phenylindole; FCCP, carbonyl cyanide 4-[trifluoromethoxy]phenylhydrazone; CL, cardiolipin; CFU, colony forming units; EB, ethidium bromide; FRET, fluorescence resonance energy transfer; YPGal, galactose, peptone and yeast extract media; YPD, glucose, peptone and yeast extract media; YPEG, glycerol, ethanol, peptone and yeast extract media; mtDNA, mitochondrial DNA; PMSF, phenylmethanesulfonyl fluoride; PC, phosphatidylcholine; PE, phosphatidylethanolamine; PG, phosphatidylglycerol; PS, phosphatidylserine; WT, wild type; TMRM, tetramethyl rhodamine, methyl ester

* Corresponding author at: Departamento de Bioquímica, IQ, Universidade de São Paulo, Av. Prof. Lineu Prestes, 748, Cidade Universitária, 05508-900 São Paulo, SP, Brazil. Tel.: +55 11 30912922.

E-mail address: aluevano@iq.usp.br (L.A. Luévano-Martínez).

http://dx.doi.org/10.1016/j.bbabio.2015.03.007
0005-2728/

and vacuolar acidification [17–19]. However, little is known to date regarding the mechanisms involved in the stabilization of mitochondrial function by CL during these non-permissive conditions.

A puzzling characteristic of CL is that, despite its described importance in several pivotal aspects of mitochondrial physiology, several model organisms tolerate the absence of this phospholipid. It has been suggested that PG and/or PE could substitute for CL under optimal growth conditions [20]. This hypothesis is confirmed by the synthetic lethality of yeast lacking both PE and CL [21] and the *petite* (respiratory-incompetent) phenotype present in mutants of the PGS1 gene, which codes for phosphatidylglycerol phosphate synthase, the rate limiting step in anionic phospholipid biosynthesis [22]. Other reports, however, have indicated that CL is required under stressful conditions, and cannot be completely replaced by these phospholipids [23–25].

Here, we directly investigate the role of CL in the cellular response to mitochondrial stress using a genetic model in which CL biosynthesis was disrupted by deleting the cardiolipin synthase gene (CRD1). This strain has been previously characterized [17,18] and accumulates PG, which is believed to replace CL in certain functions, since the cells are respiratory-competent. Interestingly, we found that while CL is not essential for respiratory function under optimal growth conditions, the biophysical properties it confers to mitochondrial membranes are essential for mtDNA stability and segregation under stress.

2. Materials and methods

2.1. Yeast strains and culture

The *Saccharomyces cerevisiae* BY4741 strain *MAT***a** *ura3*Δ0 *leu*Δ0 *met15*Δ0, its isogenic cardiolipin synthase-null strain *MAT***a** *ura3*Δ0 *leu2*Δ0 *met15*Δ0 *crd1*::G418 and BY4742 *MAT*α *ura3*Δ0 *leu2*Δ0 *lys2*Δ0 strains were used in this study.

Mitochondrial DNA loss (ρ^0) was induced in the BY4742 background by culturing in YPD broth (2% glucose, 2% peptone and 1% yeast extract) supplemented with 25 μg/mL ethidium bromide and growing until saturation. Cells were then plated in solid YPD and replica-plated on glycerol media to select for *petite* colonies. Cells were pre-cultured in respiratory media (YP broth supplemented with 2% glycerol and 3% ethanol) at 30 °C under vigorous shaking (300 rpm) to positively select against mtDNA loss. After six generations [approximately 15 h], the cells were washed and YPD (2% glucose) or YPGal (2% galactose) culture broth was inoculated at an initial optical density of 0.01 at 30 °C or 37 °C, to induce thermal stress. Growth was followed under both conditions by measuring optical density at 600 nm.

To verify the effect of intermediate levels of CL on mtDNA stability, a tet-off system coupled to the promoter region of the phosphatidylglycerol phosphate synthase (PGS1) gene was used (Dharmacon, GE Healthcare). Cells were routinely grown in YPGal until saturation and subsequently diluted to an optical density of 0.01 in fresh YPGal media incubated with the indicated concentrations of doxycycline (Dox; 2.5–7.5 μg/mL) for 2 generations to repress the expression of *PGS1*. Cellular growth was not affected by doxycycline supplementation (not shown).

2.2. Mitochondrial DNA stability and hypersuppressiveness test

Aliquots of YPEG cultures at the stationary phase were diluted to a final optical density of 0.2 in distilled water and serially diluted to a final optical density of 0.0002. This last dilution was spread on solid YPD to quantify *petite* formation frequency and on solid YPEG supplemented with 50 μg/mL erythromycin to select for mtDNA mutation frequency. Under both conditions, approximately 80–100 colony forming units (CFU) of the erythromycin-resistant petite ρ^0 and ρ^- colonies were spread on YPDG medium (similar to YPD, in which both 0.5% glucose and 2% glycerol are present) and counted manually. A solution of 2% agar supplemented with 5 mg/mL phenyl tetrazolium was layered onto these plates and incubated for 3 h. Red (respiratory competent) and white/pink (respiratory incompetent) colonies were counted manually. Results are expressed as percentage of respiratory competent cells [26]. Additionally, the previous serial dilutions were spotted on YPD and YPEG plates supplemented with 2 and 4 μg/mL ethidium bromide. All plates were incubated at 30 °C or 37 °C.

The hypersuppressive respiratory phenotype was analyzed by crossing *MAT***a** — ρ^+ strains (wild type BY4741 and *crd1Δ*) with BY4742 ρ^0 (*MAT*α) cells. Briefly, strains were inoculated in YPD broth until the stationary phase. Each strain was washed and mixed at a 1/1 ratio with fresh YPD broth [27]. Mating mixtures were incubated overnight at 30 °C or 37 °C. Samples were plated on glucose minimum mineral media lacking methionine and lysine to select for diploid cells. Afterward, the plates were layered with tetrazolium solution to count for respiratory suppressiveness in colonies.

2.3. mtDNA copy number detection

A 147 bp size fragment within the *COXI* mtDNA gene was amplified using the primer sequences: forward 5′-CTACA GATACAGCATTTCCAA GA-3′ and reverse 5′-TGCCTGAATAGATGATAATGGT-3′. Mitochondrial DNA copy number was normalized to the amplification of the nuclear single copy gene *ACT1*, which was amplified using the following primers: forward primer 5′-GTATGTGTAAA GCCGGTTTTG-3′, and reverse primer 5′-CATGATACCTTGGTGTCTTGG-3′. Primer design was performed using Primer Express 2.0 software (Applied Biosystems). Real-time PCR amplification was performed in 25 μL containing 1 × TaqMan Universal PCR Master Mix with SYBR green (Applied Biosystems), 100 nM of each primer, and 1–10 μL DNA extract. The thermal cycling conditions were 95 °C for 10 min, 45 cycles at 95 °C for 15 s and 60 °C for 1 min. The correct amplification of the desired products was confirmed by sequencing. At least three "no-template-controls" were included in each experiment. The comparative Ct method was applied for quantification of the mitochondrial DNA copy number [28].

2.4. Isolation of yeast mitochondria

Mitochondria were isolated from galactose-grown cultures after enzymatic treatment of cell cultures [29]. Briefly, cells from 500 mL cultures were washed in pre-chilled distilled water and diluted to a final concentration of 0.25 mg/mL in zymolyase buffer (1.3 M sorbitol, 10 mM EDTA, 20 mM HEPES pH 7, 10 mM β-mercaptoethanol) supplemented with 2 mg/g_{cell} zymolyase and incubated for 40 min at 30 °C with intermittent shaking. After incubation, spheroplasts were washed in isolation buffer (0.6 M mannitol, 10 mM EDTA, 20 mM HEPES pH 7, 0.2% BSA). Pelleted spheroplasts were diluted in 10 mL of the same buffer and broken with 20 strokes of a Dounce homogenizer with a tight pestle. Mitochondria were then isolated by differential centrifugation [30]. Isolated mitochondria were assayed for coupling and integrity by following oxygen consumption and responses to ADP and oligomycin. Typical preparations yield approximately 100 mg of mitochondrial protein from 2 g (dry weight) of cells. Protein was quantified by the Bradford method.

2.5. Respiratory activity

Cellular and mitochondrial oxygen consumption was measured in an Oroboros high-resolution oxygraph at 30 °C as in [31] using absolute ethanol (1 μL/mL) as respiratory substrate. The uncoupler FCCP was added at a final concentration of 10 μM for cells and 1 μM for isolated mitochondria, where indicated.

Activities of cytochrome *bc*1 (complex III) and cytochrome *c* oxidase (complex IV) were quantified by cytochrome *c* reduction and oxidation, respectively [32,33]. Briefly, for complex III activity, mitochondria were diluted to a final concentration of 0.5 mg/mL in a buffer composed of 0.6 M mannitol, 20 mM HEPES pH 7, 0.01% Triton X-100, 50 μM potassium cyanide and 20 μM yeast cytochrome *c*. The reaction was

initiated by the addition of 5 μM reduced coenzyme Q_2, and cytochrome *c* absorbance was followed with a DW200/Aminco Ollis spectrophotometer in double-beam mode at 550–535 nm [32] using a molar extinction coefficient for cytochrome *c* of 21.5 mM^{-1} cm^{-1}. Reduced coenzyme Q_2 was chosen as a substrate because of its higher solubility in polar solvents compared to ubiquinone (Q_{10}). Commercially available coenzyme Q_2 was dissolved in absolute ethanol. The ethanolic solution of Q_2 was dissolved in 10 mL of 20 mM PBS buffer, pH 7, sodium borohydride was added until hydrogen production was exhausted, and subsequently solid sodium dithionite was added until the orange color disappeared completely. Reduced coenzyme Q_2 was extracted by five successive washes with ultrapure n-hexane. The organic phase was nitrogen-dried and dissolved in 1 mL methanol containing 10 mM HCl. Reduced coenzyme Q_2 concentration was measured at 268 nm using a molar extinction coefficient of 15,162 mol^{-1} cm^{-1} [33].

Complex IV activity was measured following reduced cytochrome *c* oxidation [34]. Solid yeast cytochrome *c* (20 mg) was dissolved in 1 mL 20 mM HEPES pH 7 and small amounts of sodium dithionite were added to reduced cytochrome *c* until the 550/535 nm absorbance ratio was equal to or higher than 6. Mitochondria were diluted at 0.5 mg/mL in 0.6 M mannitol, 20 mM HEPES pH 7 and 5 μg/mL antimycin A. The reaction was started by adding 20 μM reduced yeast cytochrome *c*. Cytochrome *c* oxidation was measured in a DW200/Aminco Ollis spectrophotometer in double-beam mode at 550–535 nm [34]. The molar extinction coefficient used for cytochrome *c* was 21.5 mM^{-1} cm^{-1}. Alternatively, cytochrome *c* oxidase was quantified polarographically in an Oroboros oxygraph. Mitochondria were diluted at 0.5 mg/mL in isolation buffer supplemented with 5 μg/mL antimycin A and 20 mM ascorbate. The reaction was initiated by the addition of 100 μM TMPD.

Citrate synthase activity was measured as in reference [34]. This activity was used to normalize specific activities of complexes III and IV to mitochondrial content. Proteins were resolved by SDS-PAGE in a 12% acrylamide gel and transferred to PVDF membranes. Expression of mitochondrial-coded cytochrome *c* oxidase subunit II was measured using standard Western blotting techniques and a 1:5000 dilution of COXII antibody (Abcam, Cambridge, UK). Protein was quantified by the Bradford method.

2.6. Mitochondrial cytochrome content

Freshly isolated mitochondria were diluted to a final concentration of 3 mg/mL in 0.6 M mannitol, 20 mM HEPES, and 0.05% sodium deoxycholate (sample absorbance of 1–1.5). Oxidized and reduced spectra were determined by adding a small amount of ferricyanide and sodium dithionite, respectively. Oxidized to reduced differential spectra were determined in a DW200/Ollis Aminco spectrophotometer in split mode. Intensities of the α-bands were scanned from 500 to 650 nm [35]. Cytochrome content was obtained from these differential spectra from the difference between maxima and the respective isosbestic absorbance. The extinction coefficients used were: $\Delta\varepsilon_{550-540} = 18{,}700\ M^{-1}$ for cytochromes *c* (*c* + *c1*), $\Delta\varepsilon_{560-575} = 23{,}400\ M^{-1}$ for cytochromes *b* and $\Delta\varepsilon_{603-630} = 24{,}000\ M^{-1}$ for cytochromes *a* + *a*3 [36].

2.7. Phospholipid analysis

Phospholipids were extracted from isolated mitochondria by a modification of the Bligh & Dyer method [36]. Briefly, 500 μL of the mitochondrial suspension was incubated with 1 mL 0.1 N HCl, 2 mL methanol and 1 mL chloroform. The mixture was incubated for 30 min with intermittent mixing. Subsequently, 2 mL of a 1:1 mixture of 0.1 N HCl:chloroform was added. The emulsion was broken by centrifugation at 2000 rpm for 20 min. The upper water phase was aspired and the organic phase was nitrogen-dried. Dried lipids were dissolved in 100 μL of chloroform:isopropanol (1:1). A 50 μL aliquot was used for phosphorus determination by the Fiske & Subbarow method [37].

Qualitative analysis of mitochondrial phospholipids was performed by thin layer chromatography. Phospholipids (300 nmol by phosphorous) were applied on a Kieselguhr silica matrix pre-treated with 1.8% boric acid. Plates were baked for 1 h at 100 °C. Samples were developed in chloroform:methanol:NH_4OH (28% solution):H_2O (60:37.5:3:1). Spots were visualized by iodine staining and analyzed by densitometry [38]. Individual phospholipids were scraped from the TLC plate and assayed for phosphorous content. The mol fraction of CL, PG, PE and PC was calculated by the proportion between phosphorous for individual phospholipids and total phosphorous (300 nmol) [38].

2.8. Membrane surface charge and flexibility assays

Surface charge was qualitatively monitored by ANSA fluorescence. ANSA increases its quantum yield in lipid environments. It is assumed to bind preferentially to zwitterionic or neutral phospholipids. For the assay, 0.5 mg/mL mitochondria were incubated in isolation buffer previously treated with a cationic exchange resin. Emission scanning with excitation at 385 nm was initiated by the addition of 15 μM ANSA to the mitochondrial suspension. Maximal fluorescence intensity was attained by the addition of 50 μM $CaCl_2$, which interacts with anionic phospholipids, thus increasing ANSA affinity for membranes [39]. Phospholipid headgroup hydration was measured by the emission generalized polarization of laurdan (6-dodecanoyl-2-dimethylaminonaphthalene). Mitochondria were diluted in isolation buffer at 0.5 mg/mL and incubated with 1 μM laurdan. The probe was excited at 340 nm and emission intensity at 440 and 490 nm was recorded at 30 °C [40].

2.9. Confocal imaging

Yeast strains were grown in YPD at 30 °C or 37 °C to low log phase ($5{10}^6$/mL). The cells were washed and suspended in medium containing 2.5 μg/mL DAPI and 25 μM TMRM, both from Molecular Probes (Eugene, OR) and incubated in the dark for 1 h at room temperature. The cells (1 mL) were then centrifuged and suspended in phosphate buffer. To avoid physical damage and to hold cells in a fixed position, a pad of 2% agarose was applied directly on top of the slide and a 5 μL sample transferred to the slide and immediately covered with a coverslip. Images were obtained with a confocal total internal reflection fluorescence wide-field microscope equipped with a 100×/1.40 NA oil objective lens (Carl Zeiss). Z stacks across the depth of the cells were acquired to provide steady-state 3D information on mitochondrial morphology. Dataset projections of the z-stacks were generated and quantified with ImageJ software. All the fluorescent stacks were quantified from an average of 10 zygotes for each group at different temperatures, in at least 3 independent experiments.

2.10. Mitochondrial nucleoid isolation

Mitochondria were isolated as described above. They were then purified and incubated for 16 h in cross-linking buffer composed of 0.6 M mannitol, 20 mM HEPES pH 7.4, 1 mM spermidine, 5 mM β-mercaptoethanol, 1 mM PMSF and 1% formaldehyde. Cross-linking was stopped by adding 160 mM glycine, pH 7. Mitochondria were pelleted at 12,000 rpm for 10 min and suspended in cross-linking buffer without formaldehyde. Mitochondria were then lysed by adding 0.5% IGEPAL-40 (Sigma-Aldrich) and incubated over ice for 10 min. The solution was poured onto a sucrose gradient composed of 20, 40, 60 and 80% solutions and centrifuged. Nucleoids were recovered from the 20–60% layers. Nucleoid purification was determined by DAPI fluorescence ($\lambda_{exc} = 358$, $\lambda_{em} = 461$; [41]).

2.11. Protein-lipid overlay assay

40 μg of the indicated phospholipids (Avanti Lipids) was spotted onto a strip of PVDF membrane. Strips were nitrogen dried and

incubated in blocking buffer (50 mM Tris–HCl pH 7, 150 mM NaCl, 0.1% Tween-20, 3% BSA) for 1 h. Subsequently, each strip was incubated with same amount of cross-linked mitochondrial nucleoid solution for an additional 1 h. Phospholipid-bound nucleoids were detected by using an antibody against the nucleoid protein constituent Hsp60 (Abcam) at a dilution of 1:2000. Secondary anti-mouse antibody was used at a 1:25,000 dilution and revealed by chemioluminescence [42–44]. Nucleoids bound to the phospholipid matrix were also stained with 1 μM PAGE GelRed Nucleic acid gel stain (Biotium). mtDNA was visualized by UV imaging.

2.12. Förster resonance energy transfer (FRET) analysis

Isolated mitochondria were incubated for 5 min with 1 nM DAPI. An emission spectrum was recorded exciting at 358 (5 nm slits). After spectra recordings, 5 μM of the membrane probe 18:1 NBD-PE (1,2-oleyl-sn-glycero-3-phosphoethanolamine-N-7-nitro-2-1,3-benzoxadiazol-4-yl) from Avanti Lipids was added and incubated for a further 5 min. New emission spectra were recorded. FRET efficiency (E) was quantified using the formula: $E = I_{DA}/I_D$, where I_D refers to the fluorescence intensity of the donor alone (DAPI) and I_{DA} for the donor–acceptor (NBD-PE–DAPI) couple. FRET experiments were performed with each sample at 30 °C and 37 °C.

2.13. Statistical analysis

At least three independent experiments ($n = 3$) were performed and each replica was determined in triplicate. Data were analyzed by two-way ANOVA using Origin 7.0. A $p < 0.05$ was considered statistically significant.

3. Results

3.1. Lack of cardiolipin and thermal stress suppresses respiratory metabolism

Previous findings suggest that the lack of CL impairs respiratory maintenance in growing cells when submitted to thermal stress [19, 45]. Indeed, we found that cells deficient in cardiolipin synthase (*crd1Δ*) displayed a blunted diauxic shift when their growth curves in glucose were followed (Fig. 1A). The diauxic shift can be observed by the temporarily slower growth rate (indicated by the arrows and dotted lines) when glucose is exhausted in the media, and cells begin respiratory growth supported by mitochondrial biogenesis. At 30 °C, *crd1Δ* cells presented a dampened [32] shift compared to wild-type (WT) cells. The diauxic shift was absent at 37 °C in *crd1Δ*, but not WT cells. Although cellular respiratory rates in *crd1Δ* cells were similar to WT at 30 °C (suggesting no overall impairment of respiratory function due to the lack of CL), they were significantly decreased by thermal stress, specifically in these mutants (Fig. 1B).

The results obtained suggest that *crd1Δ* cells develop respiratory dysfunction specifically under thermal stress conditions. In order to further corroborate the hypothesis, cells were cultured in galactose media, which do not repress mitochondrial metabolism. As observed in Fig. 1C, WT and *crd1Δ* strains show similar final growth at 30 °C, although the mutant strain showed a slower growth rate. At 37 °C, *crd1Δ* cells displayed a very pronounced lag phase and a lower final optical density at the stationary phase, indicating that these cells have a temperature-sensitive defect in respiratory metabolism, independent of glucose repression.

3.2. Mitochondrial membranes are remodeled under thermal stress, in a CL-dependent manner

In order to understand why respiratory function was maintained in *crd1Δ* cells under normal growth conditions, but not under conditions of thermal stress, we analyzed the lipid content of mitochondria from these cells. Fig. 2A shows the lipid content of mitochondrial membranes under the same growth conditions as Fig. 1. As expected, *crd1Δ* cells presented no detectable levels of CL. WT cells present a very significant increase in CL under conditions of thermal stress. The CL precursor PG was not detected in WT cells, but, as expected, accumulates in *crd1Δ* mitochondria ([18], Fig. 1A). However, PG levels did not change significantly in content with thermal stress.

Mitochondria are also the major producer of another non-bilayer phospholipid, PE. We found that under thermal stress the PE also

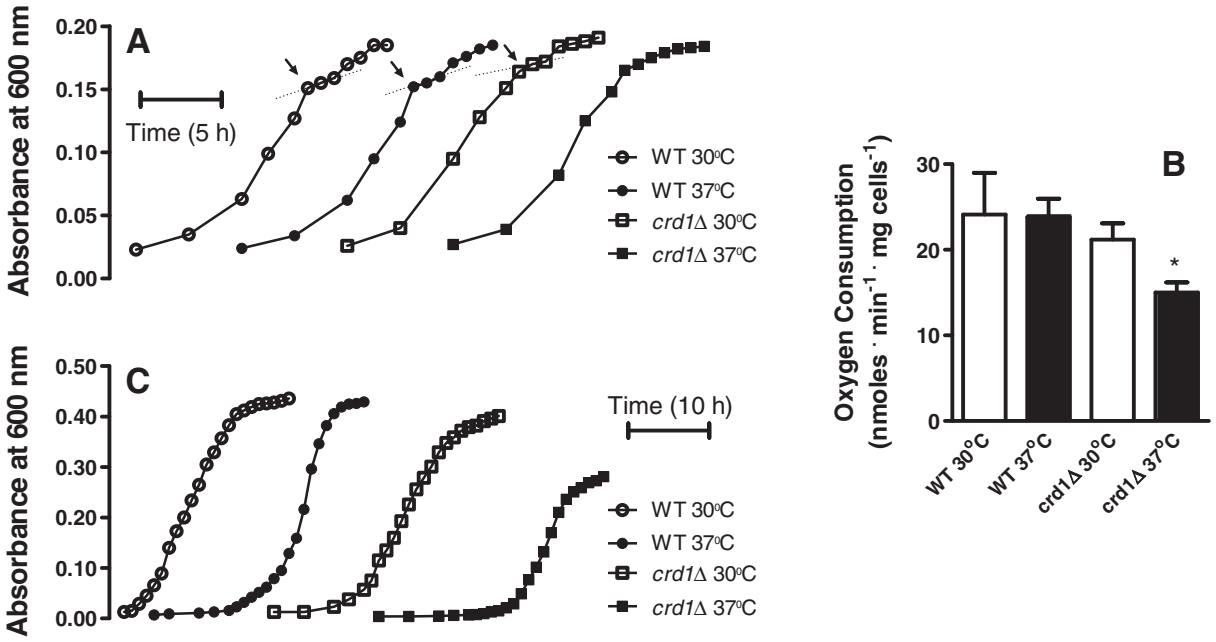

Fig. 1. CL-deficient cells do not present a typical diauxic shift and present decreased respiration under thermal stress. A) Growth kinetics in glucose complete media (YPD) were followed in WT and *crd1Δ* cells grown at 30 °C or 37 °C, as indicated. The diauxic shift is indicated by arrows and dotted lines. B) Ethanol-supported intact cell respiration at 30 °C (open bars) or 37 °C (closed bars). C) Growth kinetics in galactose were followed in WT and *crd1Δ* cells grown at 30 °C or 37 °C, as indicated. * $p < 0.05$ *versus* 30 °C. Data represent the mean value ± SEM of at least 3 experiments in triplicate.

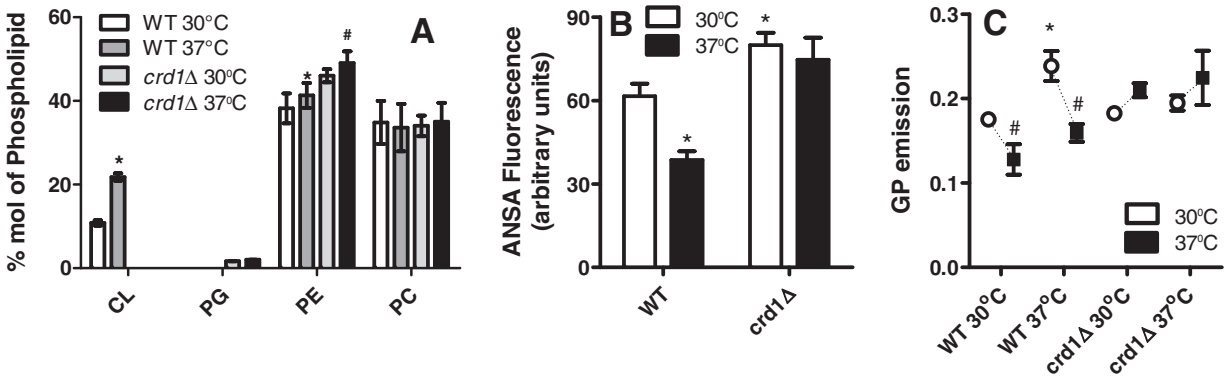

Fig. 2. Plasticity of mitochondrial membranes promoted by thermal stress requires CL. A) Mol fraction of phospholipids from isolated mitochondria of cells grown at 30 °C and 37 °C, as indicated. PG was undetectable in WT, while CL was undetectable in *crd1Δ* mitochondria. B) Surface charge of mitochondrial membranes measured by ANSA fluorescence in the presence of calcium at 30 °C (open bars) or 37 °C (closed bars). C) Generalized polarization (GP) emission of mitochondrial membranes measured at 30 °C (○) or 37 °C (■) from WT or *crd1Δ* cells grown at 30 °C or 37 °C, as indicated in the abscissa. * $p < 0.05$, relative to measurements with WT cells grown at 30 °C. # $p < 0.05$ relative to measurements at 30 °C with the same cell type and growth condition. Data represent the mean value ± SEM of at least 5 experiments in triplicate.

increased. Previously published data also showed that PE increases in the *crd1Δ* strain [20,21,46].

The functional importance of the increase in CL during thermal stress was investigated through measurements of the biophysical properties of mitochondrial membranes. Surface charge was qualitatively assessed by following the binding of the anionic probe ANSA to isolated mitochondria (Fig. 2B). This compound has increased affinity for PC-rich membranes [47]. Indeed, we found that ANSA affinity to thermally-adapted mitochondria decreased, a result that correlates with the increased CL content at 37 °C described earlier. Thus, thermoadaptation in WT cells involves an increase in surface charge. Conversely, in CL-deficient *crd1Δ* cells, ANSA fluorescence was significantly higher than WT cells, indicating lower surface charge and reflecting the lack of CL. No change in ANSA binding was observed by growth at 37 °C, demonstrating a lack of surface charge plasticity with thermal stress in cells lacking CL.

Next, phase transition was studied in mitochondrial membranes of cells grown under our experimental conditions. Phase transition changes were qualitatively assessed by laurdan polarization, which senses the hydration degree of the polar headgroup of phospholipids in biological membranes [48]. This probe presents a red shift when in membranes in liquid-crystalline phases and a blue shift in order-gel phases. Under our experimental conditions, isolated mitochondria from the four conditions tested were incubated with laurdan and assayed at 30 °C and 37 °C. Mitochondria from cells grown at 30 °C and 37 °C were assayed at both temperatures in order to measure polarization in both growth-induced and immediate (temperature change in the cuvette) thermal adaptations of the mitochondrial membranes. WT cultures grown at 30 °C were predominantly in the liquid-crystalline phase (reflected as lower generalized polarization, GP, emission, Fig. 2C), while mitochondria from WT cultures grown at 37 °C presented membranes in gel-order phase, as shown by the higher (GP) emission. When measurements of the isolated mitochondrial membranes from those cultures were repeated at 37 °C (full symbols), a notable plasticity of the membranes from WT cells, especially those grown at 37 °C, was observed, with GP shifts indicating a change to liquid-crystalline phases. On the other hand, *crd1Δ* mitochondria did not present significant changes in phase transitions when incubated at 30 °C or 37 °C, regardless of the temperature in which the cultures were grown. This result shows a lack of membrane plasticity in cells deficient in CL, and may directly affect function, since liquid-crystalline phases are leakier than gel-order phases [49].

Altogether, our results indicate that, although PG is the precursor of CL, its biophysical properties in membranes are quite different and it is not able to replace CL during thermal adaptation.

3.3. CL preserves mitochondrial electron transport function following thermal stress

Changes in membrane composition and biophysical properties such as those observed in Fig. 2 are expected to impact mitochondrial electron transfer efficiency, as suggested by the lack of a diauxic shift and lower respiratory rates observed in Fig. 1. We thus endeavored to uncover the role of CL in respiratory function during thermal stress in a more specific manner. Respiratory rates (Fig. 3A) were quantified in cells grown at 30 °C or 37 °C, in the absence or presence of the mitochondrial uncoupler FCCP, which promotes maximal respiration. Interestingly, while both basal and FCCP-induced maximal respiratory rates were similar in *crd1Δ* and WT cells, growth at 37 °C induced a significant decrease in both basal and maximal respiratory rates exclusively in *crd1Δ* cells. These data corroborate that the lack of CL, while not affecting respiration under ideal growth conditions, impairs respiration under conditions of thermal stress [19].

To investigate the cause for the decline in maximal oxygen consumption capacity, respiratory chain cytochrome spectra were quantified by differential spectrophotometry (Fig. 3B). A clear decrease in cytochrome peaks was observed in *crd1Δ* mitochondria from cells grown at 37 °C. We also found that Cox2p (measured by Western blot) in *crd1* mutants was decreased by 35% upon incubation at 37 °C (results not shown). Altogether, these results indicate that thermal stress reduces the quantities of cytochromes *b*, *c*1 and $a + a3$ in the mutant strain. Apparently the maturation of apocytochromes was not affected, since overlapping peaks were not observed in the maxima of each particular cytochrome.

In addition to quantifying cytochrome spectra, we measured the activities of complexes III and IV. Results are presented normalized to the activity of citrate synthase, a mitochondrial matrix enzyme, in order to eliminate changes in activity promoted by changes in overall mitochondrial mass [34]. We found (Fig. 3C) that thermal stress significantly compromised complex IV activity in WT cells, and had an even more pronounced effect in *crd1Δ* mitochondria. The activity of complex III was unaffected by thermoadaptation, except for the mutant strain, in which the activity is greatly decreased (Fig. 3D). The lower activity observed in the mutant strain could be directly caused by CL absence. However, *crd1Δ* mitochondria at 30 °C did not present a decrease in complex III or IV activity, despite a total lack of this phospholipid. The fact that *crd1Δ* respiration is specifically affected under stress conditions, and involves changes in respiratory chain proteins (encoded in part by mitochondrial DNA, mtDNA) suggests that the lack of CL may prime cells toward mtDNA damage.

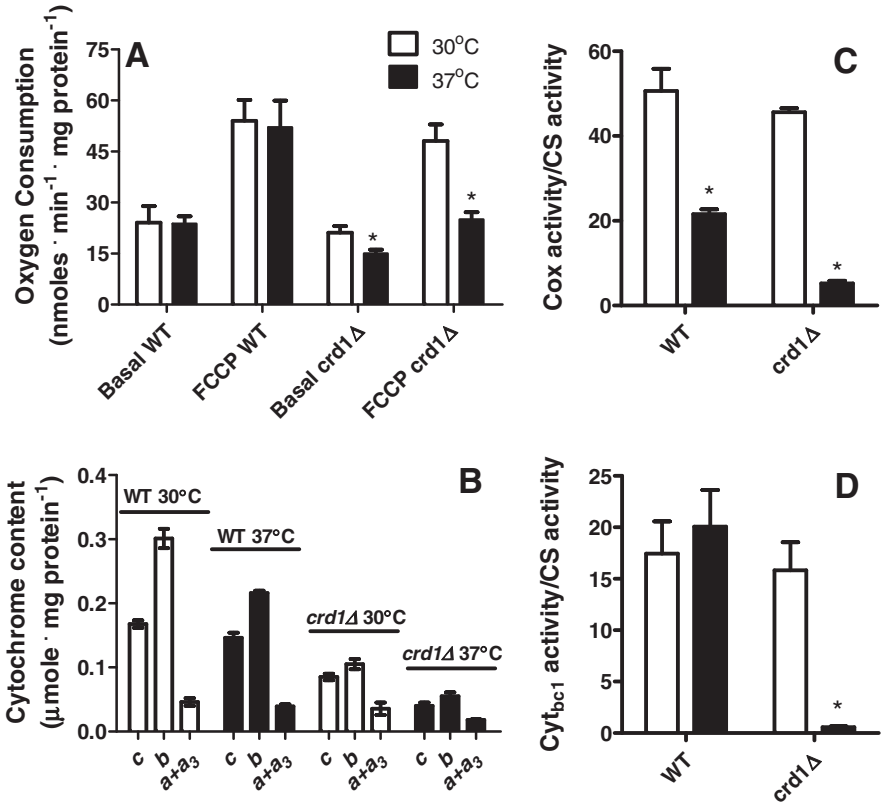

Fig. 3. CL-deficient cells lose mitochondrial respiratory proteins under conditions of thermal stress. A) Ethanol-supported mitochondrial oxygen consumption measured in WT or *crd1Δ* cells grown at 30 °C (open bars) or 37 °C (closed bars). FCCP was added where indicated to promote maximal respiratory rates. Oxygen consumption was measured at 30 °C. B) Cytochrome content from isolated mitochondria from cells grown at 30 °C (open bars) and 37 °C (full bars). C) Cytochrome *c* oxidase (Cox) activity normalized activity to citrate synthase activity from cells grown at 30 °C (open bars) or 37 °C (closed bars). D) Cytochrome *bc*1 complex activity normalized to citrate synthase activity from cells grown at 30 °C (open bars) or 37 °C (closed bars). * $p < 0.05$, relative to 30 °C. Data represent the mean value ± SEM of at least 3 experiments in triplicate.

3.4. CL protects mtDNA

The results presented until now suggest that, while the lack of CL does not directly inactivate mitochondrial respiratory activity, it leads to respiratory defects after thermal stress, characterized by the lack of respiratory chain proteins, including subunits encoded by mtDNA. This result suggests that loss of CL could promote nucleoid instability under thermal stress. To verify this possibility, ethidium bromide accessibility to the mitochondrial nucleoid was analyzed by spot testing [50]. Cells were grown in galactose media. Aliquots were serially diluted and spotted in plates containing glucose (fermentative) or glycerol/ethanol (respiratory conditions) as substrates. These plates were supplemented with increasing concentrations of ethidium bromide (Fig. 4). Under these conditions, lack of growth in respiratory media (glycerol + ethanol) demonstrates that thermal stress promotes respiratory ineptitude in both WT and *crd1Δ* cells, a condition only slightly worsened by the addition of ethidium bromide, since nucleoids are poorly accessible to ethidium bromide in respiratory media [51]. On the other hand, in glucose, CL-deficient cells were more susceptible to ethidium bromide-induced cell damage, both at permissive and non-permissive temperatures. This result suggests

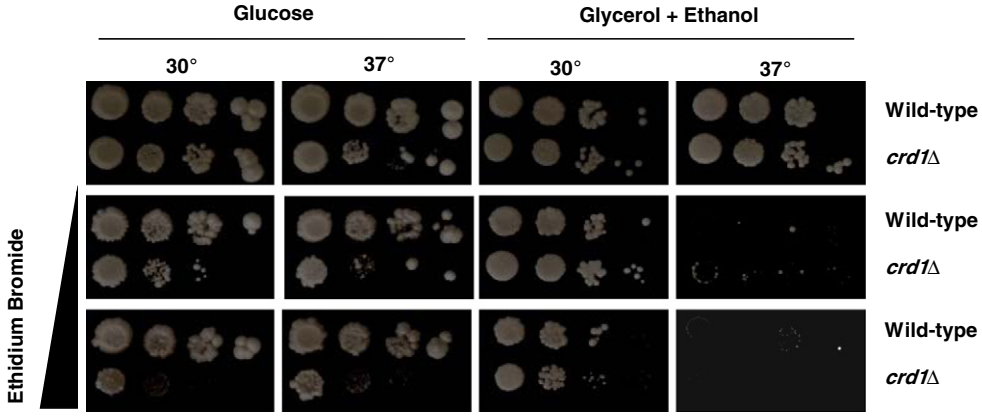

Fig. 4. CL-deficient cells are more susceptible to ethidium bromide. Cell sensitivity to ethidium bromide was assessed by spot testing as described in Materials and methods. Cells in which mtDNA is more accessible to ethidium bromide intercalation present poor growth in complete media.

that the lack of CL renders mtDNA more prone to damage under stress conditions, including both treatment with ethidium bromide and thermal stress.

3.5. CL is determinant for mtDNA inheritance

mtDNA is anchored to the mitochondrial inner membrane by protein components [52] that could have their membrane insertion affected by CL, leading to the nucleoid instability observed previously. We thus explored the stability of mtDNA more directly in CL-deficient cells. In Fig. 5A, cells were cultured under respiratory conditions to select against mtDNA loss, and transferred to glucose media in order to release selection for mtDNA maintenance. The spontaneous appearance of mtDNA-deficient *petite* colonies was then counted relative to the total amount of colonies. As observed in Fig. 5A, which quantifies respiratory competent (ρ^+) colonies, thermal stress slightly (non-significantly) decreases mtDNA stability in WT cells. Notably, cells lacking CL incubated at 37 °C produced more than 50% more *petite* colonies. This confirms the data from Fig. 4 suggesting that lack of CL promotes mtDNA instability.

To further verify if CL increases during thermoadaptation are responsible for mtDNA stability, we used a strain in which the promoter of the PGS1 gene was replaced by a tet-off system which modulates the CL/PC ratio depending on the concentration of doxycycline present in the media. This PGS1 gene was chosen because it codifies for the rate-limiting step in CL biosynthesis [53]. Data shown in Fig. 5B are expressed as a function of the measured CL/PC ratio in the mitochondria from these cells, which decreases with increasing doxycycline concentrations. While at 30 °C no effects of decreasing CL/PC ratios were observed, at 37 °C cells showed a loss of mtDNA proportional to the loss in CL. The percentage of *petite* colonies in WT cells both under permissive and thermal stress conditions was unaltered by doxycycline (results not shown). Overall, this experiment indicates that the increase in the CL/PC ratios which occurs as an adaptive response to thermal stress is responsible for stabilizing mtDNA under non-permissive conditions.

Next, we explored whether *petite* cells were produced by mtDNA loss (ρ^0) or mutations (ρ^-) in the mutant strain. This was first assessed by measuring the mtDNA content of the different strains under the same experimental conditions. We found that under respiratory conditions, the *crd1Δ* strain had 27% less mtDNA than the WT cells or the mutant strain at 30 °C (Fig. 5C). Next, we assessed mtDNA mutation rates by the appearance of erythromycin resistance, which is produced by a mutation in the mitochondrial gene of the large ribosomal subunit [54]. Strikingly, at 37 °C both WT and especially CL-deficient cells showed a much lower mutation rate when compared to 30 °C (Fig. 5D), suggesting that the *crd1Δ* strain at 37 °C produces probably ρ^0 rather than ρ^- *petites*. Together, these experiments show a decrease in mtDNA content and higher frequency of ρ^0 *petites* at 37 °C in the *crd1Δ* strain.

3.6. CL is necessary for mtDNA segregation during budding

A loss of mtDNA in dividing cells promoted by stress conditions such as those we observed could be attributable to a defect in the mitochondrial segregation apparatus during budding, resulting in decreased content of mtDNA in successive generations [55]. To test the hypothesis that CL was involved in mtDNA segregation, haploid strains (ρ^+) were crossed with a parental BY4742 strain lacking mtDNA (ρ^0) to look for a suppressive effect (see representative scheme in Fig. 6A). The rationale for this experiment was to follow the segregation of the ρ^+ genome from the WT and *crd1Δ* strains into a ρ^0 background. Cells were mated overnight and transferred to solid selecting media in order to quantify the presence of diploid *petites*. ρ^0 *versus* ρ^+ crosses within a WT

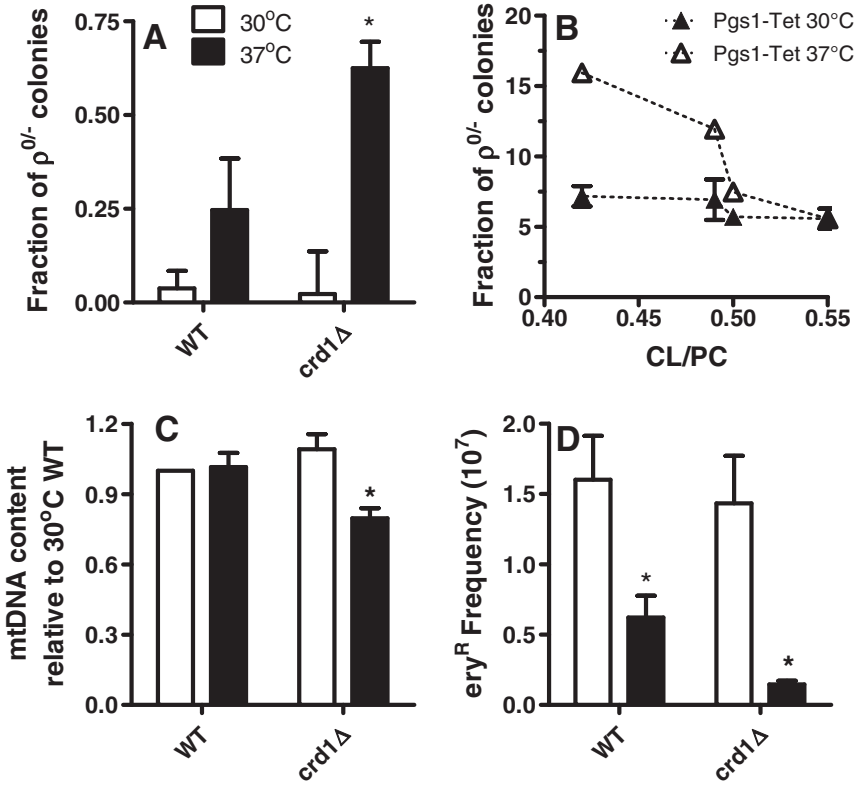

Fig. 5. mtDNA is decreased in CL-deficient cells under thermal stress. A) Respiratory competent cells grown at 30 °C (open bars) or 37 °C (closed bars) were visualized by tetrazolium staining and quantified. B) Formation of *petite* colonies as a function of the CL/PC ratio, modulated by increasing the concentration of doxycycline in a strain with a tet-off system coupled to the promoter region of the PGS1 gene. C) mtDNA content was calculated using the mitochondrial gene COX1 as a marker normalized to actin as a nuclear marker. The ratio was normalized to WT at 30 °C. D) Frequency of appearance of resistance to erythromycin. *Petite* cells showing resistance to erythromycin were visualized with tetrazolium staining in selective media supplemented with the antibiotic. * $p < 0.05$, relative to 30 °C. Data represent the mean value ± SEM of at least 5 experiments in triplicate.

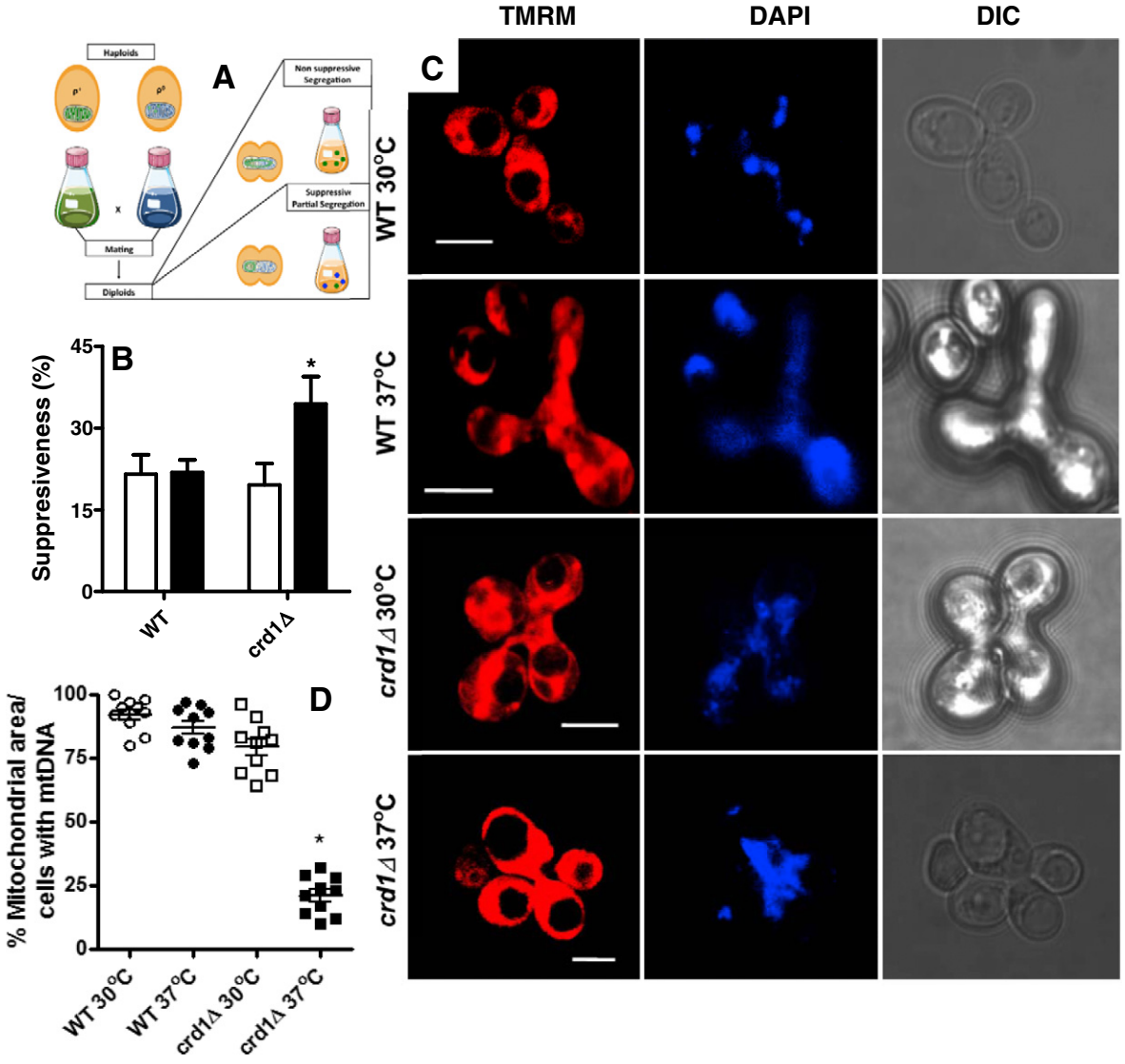

Fig. 6. CL-deficient cells have deficient mtDNA segregation under conditions of thermal stress. A) Representative scheme of the mating experimental procedure. B) Percent of respiratory incompetent ρ^0 colonies after mating at 30 °C (open bars) or 37 °C (closed bars) with WT and *crd1Δ* cells with the genotype ρ^+. * $p < 0.05$ relative to 30 °C. Data represent the mean value ± SEM of at least 5 experiments in triplicate. C) Confocal imaging of the mitochondrial network stained with TMRM and mt-nucleoid (DAPI). D) Quantification of mtDNA segregation in zygote mitochondria expressed as area of TMRM fluorescence co-localized with DAPI fluorescence in all planes of a whole specimen z-stack, data from at least 10 zygotes per group in 3 independent experiments. * $p < 0.05$ relative to 30 °C.

background (*Mat***a** ρ^+ × *Mat*α ρ^0) produced only a small proportion of respiratory suppressed cells (~25%; Fig. 6B), both at 30 °C and 37 °C. This indicates that ρ^+-WT cells were capable of distributing their mtDNA to ρ^0 cells, complementing the ρ^0 phenotype and rescuing the respiratory phenotype. On the other hand, crossing *Mat***a** *crd1Δ*$^-$$\rho^+$ *versus Mat*α WT-ρ^0 at 37 °C resulted in a 40% increase in colonies lacking respiratory capacity (Fig. 6B). This demonstrates that at non-permissive temperatures the absence of CL affects mitochondrial segregation, impairing repopulation of the ρ^0 cells with mtDNA.

In order to visually confirm the phenomenon indicated by this data, mitochondria and the distribution of mtDNA in mated cells were analyzed at permissive and non-permissive temperatures in WT and CL-lacking strains. Fig. 6C shows typical confocal microscopies in which the mitochondrial mass from both strains was marked with TMRM and mtDNA was stained with DAPI (which marks predominantly mtDNA in yeast). The images indicate that, at 37 °C, the ρ^+ genome from a *crd1Δ* strain is unable to segregate into a WT-ρ^0 strain, since DAPI fluorescence is not evenly spread among the buds (see bottom images). Interestingly, although DAPI fluorescence did not migrate within the diploid, TMRM, which marks mitochondrial membranes, did. These results are depicted in the quantification shown in Fig. 6D, which gives an indirect measure of co-localization of mitochondria and mtDNA. The results clearly indicate that CL is necessary for mtDNA migration to mated, respiratory-incompetent, cells.

To further verify that mitochondrial exchange between cells is impaired by the absence of cardiolipin, WT-ρ^0 strains were transformed with a plasmid containing a mitochondrially-tagged GFP and crossed with DAPI-stained WT and *crd1Δ* ρ^+ cells (Supplementary Fig. 1). Under these conditions, GFP-stained mitochondria were widely distributed into the zygote of WT cells. In the *crd1Δ* × WT-ρ^0 cross, GFP distribution is impaired and just a few small dot-like structures appear in the other lobules of the zygote, an effect that is strongly magnified at 37 °C. These results corroborate that mtDNA and matrix content are mixed by independent mechanisms between mitochondrial populations. Since mtDNA is anchored to the inner membrane, CL may be necessary for this lipid–nucleoid interaction and consequent mtDNA exchange.

3.7. Nucleoid–membrane binding is impaired by the lack of CL

To explore the possibility that the anchoring of mtDNA to the inner membrane was lost in the *crd1*Δ strain at 37 °C due to the lack CL, mitochondrial cross-linked nucleoids from each strain were tested for their ability to bind to different phospholipids. This experiment was done by incubating isolated nucleoids from the different yeast strains studied here with a PVDF membrane pre-loaded with purified CL, PC, PG, PE and PS (Fig. 7A). Membranes were then developed using anti-Hsp60 antibodies (leftmost strips). This protein was chosen as a target to uncover mtDNA content since it is a constitutive component of the mitochondrial nucleoid [56]. As a second form of evidencing the presence of nucleoids on our membranes (rightmost strips), a fluorescent probe for DNA (PAGE GelRed Nucleic acid gel stain; Biotium) was previously added to all nucleoid samples and detected after processing. Interestingly, using both approaches to uncover mtDNA presence, we observed that isolated nucleoids bind to CL much more significantly than PG and, to a lesser extent, PS and PE. Moreover, no significant binding was observed with PC. This experiment demonstrates that protein/DNA complexes are intact and that some component of this protein scaffold is able to interact specifically with CL. This anchorage protein (or proteins) was not apparently affected by thermal treatment since nucleoids from different strains and conditions present similar affinity toward anionic phospholipids. Since binding in all cases was stronger with CL, it can be hypothesized that during thermal stress the membranes of the CL-deficient strains show lower binding capacity to stabilize their nucleoids than WT cells.

Given the importance of these findings, which indicate a direct interaction of the mtDNA with CL, we conducted the same tests using nucleoids isolated from a mammalian cell line, in order to verify if this property is conserved (Supplementary Fig. 2). Here, the presence of the nucleoid was evidenced using antibodies against Hsp60 and mitochondrial transcription factor A (TFAM), an abundant nucleoid component. Once again, we observed that the affinity for binding to CL was much more pronounced than with any other phospholipid.

To verify if a close physical interaction exists between mitochondrial phospholipids and mtDNA within a membrane setting, isolated yeast mitochondria were stained with the DNA-specific dye DAPI and the membrane was loaded with the hydrophobic probe NBD-PE, in which a fluorescent probe is attached to the ethanolamine head group. NDB-PE is non-fluorescent in aqueous environments but, once inserted in the membrane, its quantum yield increases. We then followed the interaction of the mitochondrial inner membrane with the mtDNA/DAPI complex by FRET (typical traces are shown in Fig. 7B and quantifications in Fig. 7C). At 560 nm (where DAPI excites) NBD-PE alone presented undetectable fluorescence, but in the presence of DAPI (Fig. 7B, red line) a red shift emission particular of the NBD probe appeared, associated with a decrease in the maximal fluorescence of DAPI, as indicated by the

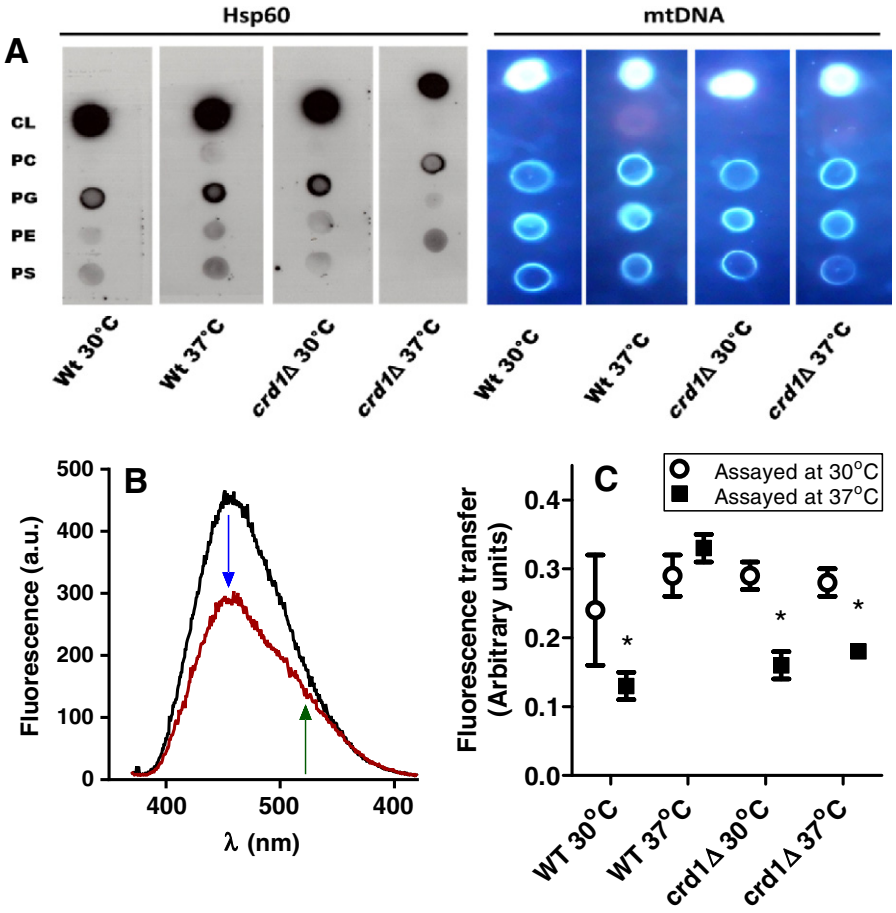

Fig. 7. Mitochondrial nucleoid binds anionic phospholipids. A) Phospholipid-nucleoid overlay assay. Purified phospholipids (50 μg) were dotted on a PVDF membrane and incubated with nucleoids isolated from cells under the conditions indicated. Associations were revealed with antibodies against the nucleoid component Hsp60 (leftmost membranes) or Gel Red (rightmost membranes, in blue). B) Representative FRET traces. WT cells were grown at 30 °C and isolated mitochondria were assayed at both 30 °C (left spectra) and 37 °C (right spectra). Green arrows indicate the fluorescence increase of the membrane NBD-PE probe after FRET. C) Quantified FRET analyses from data collected as described for panel B, at 30 °C (○) or 37 °C (■). Growth temperatures are shown in the abscissa. * $p < 0.05$ relative to the assay at 30 °C for the respective growth temperature. Data represent the mean value ± SEM of at least 3 experiments in triplicate.

arrows (black line). This result shows that energy is transferred from the DAPI/mtDNA complex to NBD-PE, and demonstrates that mtDNA is closely associated to the membrane. Fig. 7C indicates that mitochondria from the WT strain grown at 37 °C presented high transference of energy between DAPI and the membrane probe, independently of the temperature in which the assays were conducted. This demonstrates that CL-rich membranes present a closer association with mtDNA and are in line with previous reports demonstrating that this hydrophobic probe specifically stains mitochondria in proximity with nucleoid [57]. On the other hand, WT cells grown at permissive temperatures (30 °C) but assayed at non-permissive temperatures (37 °C) presented a strong decrease in the efficiency of energy transfer, suggesting that the enhanced content of CL in these cells is important for this membrane–nucleoid interaction. Conversely, the mutant *crd1Δ* strain presented low FRET efficiency when assayed at 37 °C, which indicates that CL is essential for the association of the mtDNA to the inner membrane under non-permissive conditions. Interestingly, when these mitochondrial preparations were assayed at 30 °C, they presented the same FRET efficiency as WT cells, demonstrating that mtDNA can anchor to the membrane in the absence of CL under control conditions, but not under thermal stress. Altogether, these results confirm the presence of a close physical association between the mitochondrial inner membrane and mtDNA and indicate that this association depends on the biophysical state of the membrane.

4. Discussion

In this work, we show that, while CL is not essential for respiratory function in replicating yeast cells under optimal growth conditions, it is necessary for the maintenance of mtDNA stability under conditions of stress. The protective effect of CL under stress was linked to its role in binding to mitochondrial nucleoids and guiding their segregation between cells. This allows for the maintenance of mtDNA integrity and, thus, respiratory function. The results presented here show for the first time that the biophysical properties of mitochondrial membranes conferred by CL participate in mitochondrial genomic stability and segregation.

Our findings are in line with the idea that mtDNA is tethered to the inner mitochondrial membrane by a protein–lipid complex [52], which guides the segregation of mtDNA to new cells independently of the position of the membrane itself. In prokaryotes, anionic phospholipids (PG and CL) are involved in the process of transertion (membrane protein insertion linked to co-transcriptional translation) where they transiently assist anchorage of the bacterial nucleoid to the cellular membrane [58]. Subsequently, the nucleoid is released and condensed in the protist cytoplasm. In mitochondria, it has been suggested that mtDNA is associated to the inner mitochondrial membrane through the action of several proteins in a nucleoid-like structure [59]. Since CL is constitutively synthesized in eukaryotic cells, it is tempting to conclude, based on our results, that this phospholipid is necessary for the correct association of the mitochondrial nucleoid with the inner mitochondrial membrane.

This hypothesis is supported by the fact that, under fermentative conditions (growth in glucose) in which CL biosynthesis is kept at basal levels [60], yeast cells lose mtDNA because of relaxed constraints to maintain it [61]. We also observed that in the absence of CL the mitochondrial nucleoid is easily attacked by the intercalating agent ethidium bromide, indicating that either the inner membrane composition protects mtDNA from exogenous stressors or the nucleoid association with the membrane maintains the mtDNA in a less accessible conformation, analogous to the tightly packed nucleosomes in the nucleus. Moreover, under respiring conditions (growth in glycerol + ethanol), CL content is increased, thus exerting a positive effect on mitochondrial DNA stability and segregation. Finally, we were able to show through dot-blots that isolated nucleoids from both yeast and mammal cells interact selectively with CL. Furthermore, anionic phospholipids are physically adjacent to the mtDNA, as evidenced by FRET. Finally, thin layer chromatograms of phospholipids isolated from our WT nucleoids preparations show that CL is present (results not shown), again confirming the tight association of this phospholipid with mtDNA.

The interrelationship between CL content and mtDNA was verified under thermal stress, which affects the lyotropic properties of cellular membranes due to the transition from liquid-crystalline to gel-order phase. Thermal stress increased CL biosynthesis without altering the distribution of mtDNA. This membrane remodeling [62] is absent in *crd1Δ* cells, indicating that CL, but not PG, mediates thermal adaptation. Indeed, changes in both surface charge and membrane polarization resulting from thermal stress were also absent in *crd1Δ* cells. The membrane remodeling induced by increased CL biosynthesis has functional consequences: overall mitochondrial bioenergetics was not affected in thermally-adapted WT cells, but declined in CL-deficient cells. This result is consistent with data demonstrating that surface charge is an important parameter in mitochondrial protein sorting and anchoring [63]. Although PG increases in CL-deficient cells, it is unable to exert the same adaptive response, possibly due to the differences in the physicochemical properties of this phospholipid. Moreover, a mutant *PGS1* strain, which codes for a phosphatidylglycerol phosphate synthase, is unable to retain mtDNA even under permissive conditions [64], possibly due to a disassociation process similar to that observed in our FRET experiments. The effect is similar in bacteria; an *Escherichia coli* strain lacking PG has defective transertion, which, when present, occurs in close proximity to specific membrane environments [65].

Mitochondrial dynamics are responsible for mtDNA segregation to daughter cells, producing homoplasmic offspring [66]. Our results show that adaptive responses help cells maintain normal mitochondrial morphology and dynamics, avoiding segregation defects under stress conditions. This process is strongly altered in CL-lacking cells grown in non-permissive temperatures, thus producing respiratory-defective daughters. Therefore, our results overall demonstrate that CL is pivotal in mtDNA maintenance due to its property of stabilizing the association of the mitochondrial nucleoid with the inner membrane and thus guiding segregation.

Transparency document

The Transparency document associated with this article can be found, in the online version.

Acknowledgements

This work was supported by the Fundação de Amparo à Pesquisa do Estado de São Paulo (FAPESP); grant 10/51906, Instituto Nacional de Ciência e Tecnologia de Processos Redox em Biomedicina (INCT Redoxoma), Núcleo de Apoio à Pesquisa Redoxoma (NAP Redoxoma), Centro de Pesquisa, Inovação e Difusão de Processos Redox em Biomedicina (CEPID Redoxoma) grant 13/07937-8 and the John Simon Guggenheim Memorial Foundation. We would like to gratefully acknowledge Camille Caldeira da Silva, Edson Alves Gomes and Doris Araújo for their technical support. VTSA (grant 10/18254-0) is supported by a PhD fellowship from FAPESP. LALM (grant 13/04919-9) and MFF (grant 13/04871-6) are supported by postdoctoral FAPESP fellowships. The authors have no conflict of interests to declare.

Appendix A. Supplementary data

Supplementary data to this article can be found online at http://dx.doi.org/10.1016/j.bbabio.2015.03.007.

References

[1] P. Fagone, S. Jackowski, Phosphatidylcholine and the CDP–choline cycle, Biochim. Biophys. Acta 1831 (2013) 523–532.
[2] G. Li, S. Chen, M.N. Thompson, M.L. Greenberg, New insights into the regulation of cardiolipin biosynthesis in yeast: implications for Barth syndrome, Biochim. Biophys. Acta 1771 (2007) 432–441.
[3] A.K. Menon, V.L. Stevens, Phosphatidylethanolamine is the donor of the ethanolamine residue linking a glycosylphosphatidylinositol anchor to protein, J. Biol. Chem. 267 (1992) 15277–15280.
[4] P. Rockenfeller, M. Koska, F. Pietrocola, N. Minois, O. Knittelfelder, V. Sica, J. Franz, D. Carmona-Gutierrez, G. Kroemer, F. Madeo, Phosphatidylethanolamine positively regulates autophagy and longevity, Cell Death Differ. 22 (2015) 499–508.
[5] M.G. Baile, Y.W. Lu, S.M. Claypool, The topology and regulation of cardiolipin biosynthesis and remodeling in yeast, Chem. Phys. Lipids 3084 (2013) 136–139.
[6] M. Dezi, F. Francia, A. Mallardi, G. Colafemmina, G. Palazzo, G. Venturoli, Stabilization of charge separation and cardiolipin confinement in antenna–reaction center complexes purified from *Rhodobacter sphaeroides*, Biochim. Biophys. Acta 1767 (2007) 1041–1056.
[7] V.M. Gohil, M.L. Greenberg, Mitochondrial membrane biogenesis: phospholipids and proteins go hand in hand, J. Cell Biol. 184 (2009) 469–472.
[8] B. Hoffmann, A. Stöckl, M. Schlame, K. Beyer, M. Klingenberg, The reconstituted ADP/ATP carrier activity has an absolute requirement for cardiolipin as shown in cysteine mutants, J. Biol. Chem. 269 (1994) 1940–1944.
[9] T. Hoang, M.D. Smith, M. Jelokhani-Niaraki, Expression, folding, and proton transport activity of human Uncoupling Protein-1 (UCP1) in lipid membranes: evidence for associated functional forms, J. Biol. Chem. 288 (2013) 36244–36258.
[10] D. Acehan, A. Malhotra, Y. Xu, M. Ren, D.L. Stokes, M. Schlame, Cardiolipin affects the supramolecular organization of ATP synthase in mitochondria, Biophys. J. 100 (2011) 2184–2192.
[11] M. Zhang, E. Mileykovskaya, W. Dowhan, Cardiolipin is essential for organization of complexes III and IV into a supercomplex in intact yeast mitochondria, J. Biol. Chem. 280 (2005) 29403–29408.
[12] I. Arechaga, Membrane invaginations in bacteria and mitochondria: common features and evolutionary scenarios, J. Mol. Microbiol. Biotechnol. 23 (2013) 13–23.
[13] A. Ortiz, J.A. Killian, A.J. Verkleij, J. Wilschut, Membrane fusion and the lamellar-to-inverted-hexagonal phase transition in cardiolipin vesicle systems induced by divalent cations, Biophys. J. 77 (1999) 2003–2014.
[14] N. Khalifat, N. Puff, S. Bonneau, J.B. Fournier, M.I. Angelova, Membrane deformation under local pH gradient: mimicking mitochondrial cristae dynamics, Biophys. J. 95 (2008) 4924–4933.
[15] T. Romantsov, Z. Guan, J.M. Wood, Cardiolipin and the osmotic stress responses of bacteria, Biochim. Biophys. Acta 1788 (2009) 2092–2100.
[16] R. Saxena, N. Fingland, D. Patil, A.K. Sharma, E. Crooke, Crosstalk between DnaA protein, the initiator of *Escherichia coli* chromosomal replication, and acidic phospholipids present in bacterial membranes, Int. J. Mol. Sci. 14 (2013) 8517–8537.
[17] V. Koshkin, M.L. Greenberg, Oxidative phosphorylation in cardiolipin-lacking yeast mitochondria, Biochem. J. 347 (2000) 687–691.
[18] F. Jiang, M.T. Ryan, M. Schlame, M. Zhao, Z. Gu, M. Klingenberg, N. Pfanner, M.L. Greenberg, Absence of cardiolipin in the crd1 null mutant results in decreased mitochondrial membrane potential and reduced mitochondrial function, J. Biol. Chem. 275 (2000) 22387–22394.
[19] Q. Zhong, V.M. Gohil, L. Ma, M.L. Greenberg, Absence of cardiolipin results in temperature sensitivity, respiratory defects, and mitochondrial DNA instability independent of pet56, J. Biol. Chem. 279 (2004) 32294–32300.
[20] A.S. Joshi, M.N. Thompson, N. Fei, M. Hüttemann, M.L. Greenberg, Cardiolipin and mitochondrial phosphatidylethanolamine have overlapping functions in mitochondrial fusion in *Saccharomyces cerevisiae*, J. Biol. Chem. 287 (2012) 17589–17597.
[21] V.M. Gohil, M.N. Thompson, M.L. Greenberg, Synthetic lethal interaction of the mitochondrial phosphatidylethanolamine and cardiolipin biosynthetic pathways in *Saccharomyces cerevisiae*, J. Biol. Chem. 280 (2005) 35410–35416.
[22] M. Janitor, J. Subík, Molecular cloning of the PEL1 gene of *Saccharomyces cerevisiae* that is essential for the viability of petite mutants, Curr. Genet. 24 (1993) 307–312.
[23] B. Pineau, M. Bourge, J. Marion, C. Mauve, F. Gilard, L. Maneta-Peyret, P. Moreau, B. Satiat-Jeunemaître, S.C. Brown, R. De Paepe, A. Danon, The importance of cardiolipin synthase for mitochondrial ultrastructure, respiratory function, plant development, and stress responses in *Arabidopsis*, Plant Cell 25 (2013) 4195–4208.
[24] M. Tsai, R.L. Ohniwa, Y. Kato, S.L. Takeshita, T. Ohta, S. Saito, H. Hayashi, K. Morikawa, *Staphylococcus aureus* requires cardiolipin for survival under conditions of high salinity, BMC Microbiol. 11 (2011) 13–25.
[25] L. Böttinger, S.E. Horvath, T. Kleinschroth, C. Hunte, G. Daum, N. Pfanner, T. Becker, Phosphatidylethanolamine and cardiolipin differentially affect the stability of mitochondrial respiratory chain supercomplexes, J. Mol. Biol. 423 (2012) 677–686.
[26] M. Ogur, R.St. John, S. Nagai, Tetrazolium overlay technique for population studies of respiration deficiency in yeast, Science 125 (1957) 928–929.
[27] F. Sherman, I.B. Ephrussi, The relationship between respiratory deficiency and suppressiveness in yeast as determined with segregational mutants, Genetics 47 (1962) 695–700.
[28] S.D. Taylor, H. Zhang, J.S. Eaton, M.S. Rodeheffer, M.A. Lebedeva, T.W. O'Rourke, W. Siede, G.S. Shadel, The conserved Mec1/Rad53 nuclear checkpoint pathway regulates mitochondrial DNA copy number in *Saccharomyces cerevisiae*, Mol. Biol. Cell 16 (2005) 3010–3018.
[29] M. Kozłowski, W. Zagórski, Stable preparation of yeast mitochondria and mitoplasts synthesizing specific polypeptides, Anal. Biochem. 172 (1988) 382–391.
[30] E. Zinser, G. Daum, Isolation and biochemical characterization of organelles from the yeast, *Saccharomyces cerevisiae*, Yeast 11 (1995) 493–536.
[31] L.A. Luévano-Martínez, P. Appolinario, S. Miyamoto, S. Uribe-Carvajal, A.J. Kowaltowski, Deletion of the transcriptional regulator opi1p decreases cardiolipin content and disrupts mitochondrial metabolism in *Saccharomyces cerevisiae*, Fungal Genet. Biol. 60 (2013) 150–158.
[32] E.B. Gutierrez-Cirlos, B.L. Trumpower, Inhibitory analogs of ubiquinol act anticooperatively on the yeast cytochrome bc1 complex. Evidence for an alternating, half-of-the-sites mechanism of ubiquinol oxidation, J. Biol. Chem. 277 (2002) 1195–1202.
[33] B.L. Trumpower, C.A. Edwards, Purification of a reconstitutively active iron–sulfur protein (oxidation factor) from succinate-cytochrome c reductase complex of bovine heart mitochondria, J. Biol. Chem. 254 (1979) 8697–8706.
[34] M. Spinazzi, A. Casarin, V. Pertegato, L. Salviati, C. Angelini, Assessment of mitochondrial respiratory chain enzymatic activities on tissues and cultured cells, Nat. Protoc. 7 (2012) 1235–1246.
[35] D. Lloyd, B. Chance, The cytochromes of mitochondria from *Tetrahymena pyriformis* strain ST, Biochem. J. 128 (1972) 1171–1182.
[36] E.G. Bligh, W.J. Dyer, A rapid method of total lipid extraction and purification, Can. J. Biochem. Physiol. 37 (1959) 911–917.
[37] C.H. Fiske, Y. Subbarow, The colorimetric determination of phosphorous, J. Biol. Chem. 66 (1925) 375–400.
[38] B.K. Tan, M. Bogdanov, J. Zhao, W. Dowhan, C.R. Raetz, Z. Guan, Discovery of a cardiolipin synthase utilizing phosphatidylethanolamine and phosphatidylglycerol as substrates, Proc. Natl. Acad. Sci. U. S. A. 109 (2012) 16504–16509.
[39] D.E. Robertson, H. Rottenberg, Membrane potential and surface potential in mitochondria. Fluorescence and binding of 1-anilinonaphthalene-8-sulfonate, J. Biol. Chem. 258 (1983) 11039–11048.
[40] T. Parasassi, G. De Stasio, G. Ravagnan, R.M. Rusch, E. Gratton, Quantitation of lipid phases in phospholipid vesicles by the generalized polarization of Laurdan fluorescence, Biophys. J. 60 (1991) 179–189.
[41] B.A. Kaufman, S.M. Newman, R.L. Hallberg, C.A. Slaughter, P.S. Perlman, R.A. Butow, In organello formaldehyde crosslinking of proteins to mtDNA: identification of bifunctional proteins, Proc. Natl. Acad. Sci. U. S. A. 97 (2000) 7772–7777.
[42] B.A. Kaufman, J.E. Kolesar, P.S. Perlman, R.A. Butow, A function for the mitochondrial chaperonin Hsp60 in the structure and transmission of mitochondrial DNA nucleoids in *Saccharomyces cerevisiae*, J. Cell Biol. 163 (2003) 457–461.
[43] S.V. Consonni, M. Gloerich, E. Spanjaard, J.L. Bos, cAMP regulates DEP domain-mediated binding of the guanine nucleotide exchange factor Epac1 to phosphatidic acid at the plasma membrane, Proc. Natl. Acad. Sci. U. S. A. 109 (2012) 3814–3819.
[44] D.F. Bogenhagen, D. Rousseau, S. Burke, The layered structure of human mitochondrial DNA nucleoids, J. Biol. Chem. 283 (2008) 3665–3675.
[45] F. Jiang, Z. Gu, J.M. Granger, M.L. Greenberg, Cardiolipin synthase expression is essential for growth at elevated temperature and is regulated by factors affecting mitochondrial development, Mol. Microbiol. 31 (1999) 373–379.
[46] F. Jiang, H.S. Rizavi, M.L. Greenberg, Cardiolipin is not essential for the growth of *Saccharomyces cerevisiae* on fermentable or non-fermentable carbon sources, Mol. Microbiol. 26 (1997) 481–491.
[47] J. Slavík, Anilinonaphthalene sulfonate as a probe of membrane composition and function, Biochim. Biophys. Acta 694 (1982) 1–25.
[48] F.M. Harris, K.B. Best, J.D. Bell, Use of laurdan fluorescence intensity and polarization to distinguish between changes in membrane fluidity and phospholipid order, Biochim. Biophys. Acta 1565 (2002) 123–128.
[49] J.H. Crowe, L.M. Crowe, F.A. Hoekstra, Phase transitions and permeability changes in dry membranes during rehydration, J. Bioenerg. Biomembr. 21 (1989) 77–91.
[50] J.J. Lawrence, M. Daune, Ethidium bromide as a probe of conformational heterogeneity of DNA in chromatin. The role of histone H1, Biochemistry 15 (1976) 3301–3307.
[51] X.J. Chen, X. Wang, B.A. Kaufman, R.A. Butow, Aconitase couples metabolic regulation to mitochondrial DNA maintenance, Science 307 (2005) 714–717.
[52] A.E. Hobbs, M. Srinivasan, J.M. McCaffery, R.E. Jensen, Mmm1p, a mitochondrial outer membrane protein, is connected to mitochondrial DNA (mtDNA) nucleoids and required for mtDNA stability, J. Cell Biol. 152 (2001) 401–410.
[53] S.A. Minskoff, M.L. Greenberg, Phosphatidylglycerophosphate synthase from yeast, Biochim. Biophys. Acta 1348 (1997) 187–191.
[54] F. Sor, H. Fukuhara, Erythromycin and piramycin resistance mutations of yeast mitochondria: nature of the rib2 locus in the large ribosomal RNA gene, Nucleic Acids Res. 12 (1984) 8313–8318.
[55] L. Solieri, Mitochondrial inheritance in budding yeasts: towards an integrated understanding, Trends Microbiol. 18 (2010) 521–530.
[56] M. Kucej, B. Kucejova, R. Subramanian, X.J. Chen, R.A. Butow, Mitochondrial nucleoids undergo remodeling in response to metabolic cues, J. Cell Sci. 121 (2008) 1861–1868.
[57] A.M. Grant, P.K. Hanson, L. Malone, J.W. Nichols, NBD-labeled phosphatidylcholine and phosphatidylethanolamine are internalized by transbilayer transport across the yeast plasma membrane, Traffic 2 (2001) 37–50.

[58] K. Muchová, J. Jamroškovič, I. Barák, Lipid domains in *Bacillus subtilis* anucleate cells, Res. Microbiol. 161 (2010) 783–790.
[59] M. Albring, J. Griffith, G. Attardi, Association of a protein structure of probable membrane derivation with HeLa cell mitochondrial DNA near its origin of replication, Proc. Natl. Acad. Sci. U. S. A. 74 (1977) 1348–1352.
[60] G. Tuller, T. Nemec, C. Hrastnik, G. Daum, Lipid composition of subcellular membranes of an FY1679-derived haploid yeast wild-type strain grown on different carbon sources, Yeast 15 (1999) 1555–1564.
[61] J.Z. Meyer, P.A. Whittaker, Respiratory repression and the stability of the mitochondrial genome, Mol. Gen. Genet. 151 (1977) 333–342.
[62] J.R. Hazel, E.E. Williams, R. Livermore, N. Mozingo, Thermal adaptation in biological membranes: functional significance of changes in phospholipid molecular species composition, Lipids 26 (1991) 277–282.
[63] D. Steverding, C. Thiel, B. Kadenbach, N. Capitanio, S. Papa, Influence of surface charge on the incorporation and orientation of cytochrome c oxidase in liposomes, FEBS Lett. 257 (1989) 131–133.
[64] S.C. Chang, P.N. Heacock, E. Mileykovskaya, D.R. Voelker, W. Dowhan, Isolation and characterization of the gene (CLS1) encoding cardiolipin synthase in *Saccharomyces cerevisiae*, J. Biol. Chem. 273 (1998) 14933–14941.
[65] I. Fishov, V. Norris, Membrane heterogeneity created by transertion is a global regulator in bacteria, Curr. Opin. Microbiol. 15 (2012) 724–730.
[66] J. Nunnari, W.F. Marshall, A. Straight, A. Murray, J.W. Sedat, P. Walter, Mitochondrial transmission during mating in *Saccharomyces cerevisiae* is determined by mitochondrial fusion and fission and the intramitochondrial segregation of mitochondrial DNA, Mol. Biol. Cell 8 (1997) 1233–1242.